Pattern-triggered immunity and cell wall integrity maintenance jointly modulate plant stress responses

Timo Engelsdorf[1], Nora Gigli-Bisceglia[1], Manikandan Veerabagu[1], Joseph F. McKenna[2], Frauke Augstein[1, 3], Dieuwertje van der Does[4], Cyril Zipfel[4] and Thorsten Hamann[1]

[1] Department of Biology, Høgskoleringen 5, Realfagbygget, Norwegian University of Science and Technology, 7491 Trondheim, Norway.

[2] Department of Biology, S209A Sinclair, Gypsy Lane, Oxford Brookes University, Oxford, OX3 0BP, UK.

[3] Institute for Organismal Biology, Physiological Botany, Uppsala University, Almas Allé 5, 75651 Uppsala, Sweden.

[4] The Sainsbury Laboratory, Norwich Research Park, Norwich, NR4 7UH, UK.

Author for correspondence: Thorsten Hamann

Mail: Thorsten.hamann@ntnu.no

Tel.: + 47 918 73596096

Fax: + 47 918 73596100

Summary

All plant cells are surrounded by walls, which must often meet opposing functional requirements during plant growth and defense [1–3]. The walls meet them by activating cell wall signaling processes to modify structure/composition in a controlled manner. Such adaptive changes have been summarily described as cell wall plasticity and identified as major obstacle to knowledge-based modification of lignocellulosic biomass [4]. Plasticity requires activity of the cell wall integrity (CWI) maintenance mechanism [5,6]. This mechanism monitors the functional integrity of the cell wall and initiates compensatory processes upon cell wall damage (CWD). To date, neither the mode of action of the CWI maintenance mechanism nor its' role in immunity are understood. We investigated the mechanism in *Arabidopsis thaliana* and found that CWD caused by different means induced similar, turgor-sensitive responses, suggesting similar principles underlie all CWD responses. Genetic analysis found that the receptor-like kinase (RLK) FEI2 and the plasma membrane channel MCA1 function downstream of the RLK THE1. Phenotypic clustering with 24 genotypes identified a core group of RLKs and ion channels required for activating CWD responses. By contrast, responses are repressed by pattern-triggered immune signaling components including PEPR1 and 2, receptors for the plant immune signaling peptide *At*Pep1 [7]. *At*Pep1 application repressed CWD-induced phytohormone production in wildtype, but not in *pepr1/2* seedlings. These results suggest that pattern-triggered immunity suppresses responses triggered by the CWI maintenance mechanism through *At*Pep1 / PEPR1/2-dependent signaling. However, if pattern-triggered immunity is impaired, the repression of CWI-regulated responses is removed thus compensating for immunity impairment.

Keywords:

Plant cell wall integrity, pattern-triggered immunity, THE1, cell wall signaling, turgor perception, mechano-perception, plant cell wall, peptide signaling

Results and discussion

We used an *A. thaliana* seedling-based model system to determine how plants respond to different types of CWD and further investigate the role of turgor pressure, which has been shown to affect CWD responses [8]. CWD was generated either using isoxaben (ISX), an inhibitor of cellulose biosynthesis in primary cell walls, or Driselase, an enzyme mix from *Basidomycetes sp.* containing cell wall degrading enzymes (cellulases, laminarinases and xylanases) similar to enzymes released by pathogens during infection [9,10]. The distinctly different modes of action of ISX and Driselase enabled us to investigate plant responses to fundamentally different causes of CWD (turgor-dependent vs. enzymatic). Col-0, *isoxaben resistant1-1* (*ixr1-1, cellulose synthase a3*) and *bri1-associated receptor kinase1-5* (*bak1-5)* seedlings were analyzed. *ixr1-1* seedlings form specificity controls for ISX [11]. BAK1 is an essential co-receptor for leucine-rich repeat type pattern recognition receptors. The *bak1-5* allele is only impaired in immune response but not brassinosteroid-dependent signaling and is therefore suitable for detecting effects caused either by DAMPs generated by CWD or PAMPs (pathogen-associated molecular patterns) possibly contaminating Driselase [12]. Jasmonic acid (JA), salicylic acid (SA), callose and lignin production were used as readouts since they represent established CWD and immune responses [8]. The role of turgor pressure was assessed through co-treatments with an osmoticum (sorbitol) [8].

JA and SA levels were low in DMSO (mock)-treated Col-0 and *bak1-5* seedlings and slightly elevated in *ixr1-1* (Fig. 1A, B). ISX-treatment induced JA/SA production to different degrees in Col-0 and *bak1-5* seedlings, while as expected, no induction was observed in *ixr1-1*. Treatment with Driselase induced JA/SA production in Col-0, *bak1-5* and *ixr1-1* seedlings compared to treatment with boiled Driselase, showing that enzyme activity was required for induction. Sorbitol co-treatments reduced or prevented JA/SA induction by ISX/Driselase in all genotypes examined. Intriguingly, *ixr1-1* seedlings exhibited reduced JA/SA levels whenever treated with sorbitol, suggesting these mild hyper-osmotic treatments reduce phytohormone-inducing stress in *ixr1-1* probably caused by mildly impaired cellulose synthase function. Hormone accumulation in *bak1-5* seedlings indicates that *BAK1*-dependent DAMP/PAMP recognition is not required for these responses.

Callose deposition was induced both in ISX- and Driselase-treated Col-0 cotyledons to different degrees, reduced in *bak1-5* and not induced in *ixr1-1* seedlings, which exhibited callose depositions already under mock conditions (Fig. 1C). In ISX- and Driselase-treated Col-0 cotyledons, phloroglucinol-staining visualized lignin deposition in vasculature (ISX) and non-vascular (Driselase) tissue (Fig.1D). While ISX-treated *ixr1-1* cotyledons did not exhibit increased lignin deposition, the pattern observed in Driselase-treated *ixr1* was similar to Col-0 (Fig. S1A). *bak1-5* cotyledons exhibited lignin deposition patterns similar to ISX- or Driselase-treated Col-0. CWD-induced callose and lignin deposition were always suppressed by co-treatment with sorbitol (Fig. 1C, D, S1A).

To further investigate if a secreted compound, generated by ISX or Driselase treatment, is responsible for CWD responses, JA/SA levels were measured (i) in *ixr1-1* seedlings, which had been incubated with supernatants from Col-0 seedlings treated with ISX and (ii) in Col-0 seedlings incubated with boiled supernatants deriving from Col-0 seedlings treated with Driselase for extended periods. Seedlings exhibited JA levels only barely above the detection limit, suggesting that no secreted compound eliciting JA responses was liberated by ISX/Driselase treatment (Fig. S1B). Both supernatants deriving from treatments with active and inactive Driselase induced slight elevation of SA levels whereas active Driselase induction of SA was clearly caused by enzymatic CWD (compare Fig. 1B vs. S1C).

Expression levels of *TOUCH4* (*TCH4*) and *PLANT DEFENSIN1.2* (*PDF1.2*) were determined to assess the impact of different CWD types on expression of markers for mechanical stimulation (*TCH4*) or defense signaling (*PDF1.2*) [13,14]. *TCH4* expression was induced in Col-0 by ISX and active Driselase while sorbitol co-treatments reduced it, suggesting sensitivity to turgor manipulation and mirroring changes observed in JA/SA levels (Fig. 1E). *PDF1.2* expression was investigated in Col-0 and *bak1-5* seedlings treated with Driselase or boiled Driselase. *PDF1.2* expression was induced similarly in Col-0 seedlings regardless if Driselase was active or boiled (Fig. 1F). This suggests, that Driselase contains heat-insensitive compounds (possibly PAMPs) inducing *PDF1.2* expression (mirroring on the transcriptional level the effects observed before for SA, see Fig. S1C). *PDF1.2* expression was enhanced in Driselase-treated *bak1-5* seedlings but barely induced by boiled Driselase, suggesting that two different

processes regulate *PDF1.2* expression. One is dependent on PAMP perception through BAK1 while the other one is only detectable upon BAK1 loss.

Treatments with 300 mM sorbitol normally result in mild hyper-osmotic shocks [15]. However, here they reduce the effects of both ISX- and Driselase-treatments (Fig. 1A-E). This suggests that ISX-/Driselase-treatments have opposite effects on turgor levels compared to sorbitol. They seem to generate the equivalent of a hypo-osmotic shock by weakening cell walls while turgor pressure remains high, thus leading to turgor-based cell expansion/CWD. To test this hypothesis we monitored simultaneously epidermal cell shape and viability in seedlings expressing the WAVE131-YFP plasma membrane marker (Geldner et al. 2009) stained with propidium iodide (PI) after mock-, sorbitol-, ISX- or ISX/sorbitol-treatment (Fig. S1D). Here we simplified the experimental setup by using only ISX since in previous experiments ISX and Driselase caused similar responses and ISX is a better characterized and controllable CWD agent [10]. Sorbitol-treated seedlings exhibited minor swelling in the root tip area. ISX-treatment of seedlings resulted in swelling of epidermal cells and occasional cell death, which were both reduced upon sorbitol co-treatment (Fig. S1D).

Next, we investigated if genes implicated in mechano- (*MID1-COMPLEMENTING ACTIVITY*, *MCA1*; *MSCS-LIKE4/5/6/9/10; MSL4/5/6/9/10*), hypo-osmotic *(MSCS-LIKE2/3; MSL2/3, MCA1*) or hyper-osmotic stress (*ARABIDOPSIS HISTIDINE KINASE1*, *2*/*3*, *4*; *AHK1, AHK 2/3, AHK4*) and putatively wound perception (*GLUTAMATE-LIKE RECEPTOR 2.5*; *GLR2.5*) are required for the osmotic suppression observed [16]. *GLR2.5* was selected since it exhibits the most pronounced ISX-dependent transcriptional changes off all *GLR* genes analyzed and GLRs have been

implicated in wounding response [8,17]. We included here also the *theseus1-4* allele (*the1-4*) since *the1-4* seedlings exhibit enhanced responses to ISX-treatment, enabling us to test if stimuli perceived by the THE1 RLK (a bona fide CWI sensor) are also suppressed by osmotic support (compare results for confirmed loss-of-function *the1-1* allele vs. *the1-4* in Fig. 2) [18]. Specific details for the other genotypes used here are provided in the Key Resources Table. Mutant seedlings were mock-, ISX-, sorbitol- or ISX/sorbitol-treated and analyzed for JA accumulation and lignification in the root tip (Fig. 2, Fig. S2). Only *mca1* and *msl2/3* seedlings exhibited reduced responses to ISX-treatment alone, while in all genotypes examined osmotic suppression was still detectable. Interestingly ISX/sorbitol-treated *the1-4* seedlings also exhibited reduced responses compared to ISX alone, showing that the stimulus THE1 perceives, is turgor-sensitive. The osmotic suppression observed here could be based on turgor-equilibration processes (exemplified by the shape changes observed in the epidermal cells, see Fig. S1D) and would therefore not require any of the sensors tested [19]. The similarities in seedling responses to different types of CWD (enzymes vs. ISX) suggest that even if CWD causes differ, the stimulus activating them may be the same. Turgor manipulation affects all phenotypic CWD effects examined while supernatants from seedlings, which had experienced CWD previously, do not induce CWD responses. This suggests that turgor-sensitive, non-secreted stimuli activate CWD responses. The stimuli could be cell wall-bound epitopes changing conformation and/or mechanical distortion/displacement of the plasma membrane against the cell wall upon CWD, similar to processes observed in *Saccharomyces cerevisiae* [20].

Previously, RLKs required for cell elongation, fertilization and immunity have also been implicated in CWI maintenance [3,18,21]. To investigate, which (if any) of the candidate genes are required, we investigated KO or gain-of-function alleles for 14 RLKs (*THESEUS1* (*THE1*), *CURVY1* (*CVY1*), *FERONIA* (*FER;* knock-down allele *fer-5*), *HERCULES1* (*HERK1*), *HERCULES2* (*HERK2*), *ERULUS* (*ERU*), *WALL ASSOCIATED KINASE2* (*WAK2*), *WAK2*^{cTAP}, *FEI1*, *FEI2, MIK2*, *BAK1*, *BAK1-LIKE 1* (*BKK1*), *PEPR1*, *PEPR2* and for *BOTRYTIS-INDUCED KINASE1* (*BIK1*) and *RECEPTOR-LIKE PROTEIN44* (*RLP44*). JA/SA levels were measured in mock- and ISX-treated seedlings while root growth and ISX-resistance were also investigated to exclude indirect effects (Fig. 2A-C, Fig. S3). In parallel, we quantified lignin deposition in the root tip area using an image analysis-based approach. *fer-5* seedlings exhibited elevated JA/SA levels already in the mock-treated samples, which is in line with the multifaceted functions shown for FER (Fig. S3A-B) [18,22]. ISX-dependent responses were further increased in *fer-5*, suggesting that *FER* is not required for the perception of CWD triggered by ISX (Fig. 2A-C, Fig. S3C-D). Data for *fer-5* were not included in the following step to avoid distortion during data integration. The remaining data (incl. data for osmo-/mechano-sensor mutants) were integrated through phenotypic clustering (Fig. 2D). This generated a global, standardized overview allowing assessment of both relative importance and functions of individual candidates in CWI maintenance. The clustering results show that KOs in 5 candidates (*bak1-5*, *bkk1*, *bik1*, *pepr2*, *pepr1*) involved in pattern-triggered immunity (PTI) cause enhanced responses to ISX-treatment. While the *WAK2*^{cTAP} dominant active allele exhibits also slightly elevated responses, *wak2*, *fei2* and *mik2* seedlings exhibit reductions in the CWD responses

examined. KOs in the *Catharantus roseus* RLK1L (*Cr*RLK1L) family members *CVY1*, *HERK1* and *HERK2* exhibit enhanced responses whereas *eru* and *the1-1* seedlings exhibit reduced ones, implying functional divergence within the family. In summary, phenotypic clustering shows that *WAK2*, *MIK2*, *MCA1*, *MSL2/3, ERU*, *FEI2* and *THE1* are most important for activating CWD responses. Intriguingly they are located in plasma membrane, chloroplast and vacuole, which are particularly sensitive to turgor level changes/mechanical stimuli and several of them have been previously implicated in turgor/mechano perception [16,21].

We performed a genetic analysis to establish if plasma membrane-localized CWI components (THE1, MCA1, FEI2) are part of a single or multiple signaling cascades. JA/SA/lignin levels in ISX-treated seedlings were quantified as before (Fig. 3A-C). The levels in *mca1 fei2*, *the1-1 mca1* and *the1-1 fei2* seedlings were not additive, but similar to single mutants. Interestingly, *the1-4 mca1* and *the1-4 fei2* seedlings exhibit pronounced reductions in JA/SA and/or lignin compared to *the1-4* (Fig. 3D-F). Overall, these data suggest that MCA1 and FEI2 act downstream from THE1 in the same signaling process.

To identify transcriptionally regulated elements of the CWI maintenance mechanism, Col-0 seedlings were mock- or ISX-treated and analyzed by RNA-Seq (mock- / ISX-treated *ixr1-1* seedlings acted as control). In Col-0 seedlings treated with ISX for 1 hour, 109 transcripts exhibited statistically significant differences from mock-treated controls ($p < 0.01$, Student´s *t*-test, File S1). None of them was differentially expressed in ISX-treated *ixr1-1* seedlings. GO enrichment analysis detected an overrepresentation of genes implicated in phytohormone-dependent stress responses

(Table S1). Amongst the differentially expressed transcripts were also *PROPEP1-4*, which give rise to the immune signaling peptides *At*Pep1-4 (Fig. S4A) [23]. PEPR1 binds *At*Pep1-4 while PEPR2 binds only *At*Pep1 and 2 [23]. This observation was interesting since *pepr1* and *2* exhibit enhanced JA production upon ISX-treatment (Fig. 2A). Gene expression analysis using qRT-PCR showed that *PROPEP1* and *3* are particularly strongly induced by ISX (Fig. 3G). Expression of *PROPEP1* and *3* is still elevated in ISX-treated *the1-1* seedlings, suggesting that induction is independent of THE1 (Fig. 3H). Time course expression analysis of *PROPEP1* and *3* detected increases in expression levels over time, suggesting that *At*Pep1 and 3 accumulate during the period investigated (Fig. 3I). To investigate if *At*Pep1 can increase CWD responses (as described before for JA/SA/ethylene production during wounding) [24] Col-0 seedlings were treated with different concentrations of *At*Pep1 alone or in combination with ISX and JA/SA/lignin production investigated (Fig. 3J-L). While *At*Pep1 treatments alone did not affect SA/JA levels, lignin production was induced. Surprisingly, seedlings co-treated with ISX/*At*Pep1 exhibited *At*Pep1 concentration-dependent reductions in JA/SA levels, whereas lignin deposition seemed to be additive in ISX/*At*Pep1-treated root tips compared to roots treated with either *At*Pep1 or ISX. To exclude indirect effects and determine if the observed *At*Pep1 effects are mediated via *At*Pep1 receptors, the experiments were repeated with Col-0, *pepr1* and *2* or *pepr1/2* seedlings. ISX-induced JA/SA levels were reduced in *pepr1* and *2* seedlings upon co-treatments with *At*Pep1 as observed before (Figure 3M-N). However, this was not the case in *pepr1/2* seedlings, suggesting *At*Pep1 inhibits ISX-induced phytohormone production via PEPR1 and 2. Interestingly analysis of lignin deposition in *At*Pep1-

and/or ISX-treated seedlings showed that PEPR2 (not PEPR1) is essential for *At*Pep1-induced lignin deposition, suggesting differences in signaling activities between PEPR1 and 2.

The results presented here (together with already existing literature) lead to the model shown in Figure 4. Plants perceive CWD through the CWI maintenance mechanism and PTI. The CWI maintenance mechanism involves a core group of RLKs and ion-channels located at the plasmamembrane, in the chloroplast and vacuole, enabling plant cells to detect mechanical damage to their cell walls or the consequences (Fig. 4, blue elements) [16,18,21,25]. The members of this core group probably activate Ca^{2+}-based signaling processes (based on results from previous inhibitor studies), which induce production of ROS, JA and SA [26]. Changes in phytohormone and ROS levels in turn modulate downstream responses (including lignin and callose production). While CWI maintenance has originally been only implicated in developmental processes, more recently cell wall signaling and maintenance RLKs have also been implicated in pathogen response in Arabidopsis and rice, suggesting the mechanism is active whenever plant CWI is impaired (van der Does' et al., in press) [27].

PTI is probably activated by release of *At*Pep1 in response to CWD. This event initiates immune signaling and controls the magnitude of responses activated by the CWI maintenance mechanism over time (Figure 4, red elements). This is supported by *PROPEP1* induction (encoding the precursor for *At*Pep1) in ISX-treated seedlings, which appears independent of CWI monitoring since *PROPEP1* expression is induced similarly in ISX-treated Col-0 and *the1-1* seedlings. PTI seems to limit CWI-based

induction of stress responses because on one hand *At*Pep1 application represses CWD-induced responses in a concentration- and PEPR1/2-dependent manner. On the other hand impairing other signaling elements of PTI (BAK1/BKK1/BIK1) enhances CWI-induced responses. This suggests that during early exposure to CWD both mechanisms (PTI and CWI maintenance) are activated in plants. If damage persists (ie. due to continued pathogen infection involving cell wall breakdown) activation of PTI is enhanced through an *At*Pep1-based positive feedback loop [23]. Simultaneously the same feedback loop represses the activity of the CWI maintenance mechanism, because it is not required anymore to activate defense responses. This also suggests, that the CWI maintenance mechanism can function as backup system providing basal broad-spectrum defense in case PTI is impaired (since repression of CWI signaling is removed). To summarize, our results presented here suggest that plant cells use pattern-triggered immunity and the CWI maintenance mechanism to detect CWD and modulate responses to it in an adaptive manner. Future challenges include identifying stimuli of THE1-dependent CWD signaling and elucidating the regulatory mechanisms coordinating CWI maintenance with PTI.

Author contributions

T.E., N.GB., M.V., T.H. contributed to experimental design, generated data and co-wrote the manuscript. J.McK and F.A. contributed with experimental data and to the writing of the manuscript. D.D. and C.Z. provided unpublished resources and contributed to the writing of the manuscript.

Acknowledgements

The authors would like to thank Martin Kuiper for constructive comments. Financial and/or technical support from the Deutsche Forschungsgemeinschaft EN 1071/1-1, HORIZON2020 (SugarOsmoSignaling) (T.E.), BBSRC (J.F. McK.), NTNU (M.V.), EEA grant 7F14155 CYTOWALL (N.G.B./T.H.) and the PROMEC and GCF Facilities at NTNU are gratefully acknowledged. Data generated in the transcriptomics experiments is being deposited with the Bio-analytic Resource for Plant Biology.

1. Houston, K., Tucker, M.R., Chowdhury, J., Shirley, N., and Little, A. (2016). The Plant Cell Wall: A Complex and Dynamic Structure As Revealed by the Responses of Genes under Stress Conditions. Front. Plant Sci. *7*, 1–18.
2. Somssich, M., Khan, G.A., and Persson, S. (2016). Cell Wall Heterogeneity in Root Development of Arabidopsis. Front. Plant Sci. *7*, 1242.
3. Malinovsky, F.G., Fangel, J.U., and Willats, W.G.T. (2014). The role of the cell wall in plant immunity. Front. Plant Sci. *5*, 178.
4. Doblin, M.S., Johnson, K.L., Humphries, J., Newbigin, E.J., and Bacic, A.T. (2014). Are designer plant cell walls a realistic aspiration or will the plasticity of the plant's metabolism win out? Curr. Opin. Biotechnol. *26C*, 108–114.
5. Wolf, S., Hématy, K., and Höfte, H. (2012). Growth control and cell wall signaling in plants. Annu. Rev. Plant Biol. *63*, 381–407.
6. Hamann, T. (2015). The plant cell wall integrity maintenance mechanism-concepts for organization and mode of action. Plant Cell Physiol. *56*, 215–23.
7. Yamaguchi, Y., Huffaker, A., Bryan, A.C., Tax, F.E., and Ryan, C.A. (2010). PEPR2 is a second receptor for the Pep1 and Pep2 peptides and contributes to defense responses in Arabidopsis. Plant Cell *22*, 508–522.
8. Hamann, T., Bennett, M., Mansfield, J., and Somerville, C. (2009). Identification of cell-wall stress as a hexose-dependent and osmosensitive regulator of plant responses. Plant J *57*, 1015–1026.
9. Lorences, E.P., and Fry, S.C. (1994). Sequencing of xyloglucan oligosaccharides by partial Driselase digestion: The preparation and quantitative and qualitative analysis of two new tetrasaccharides. Carbohydr. Res. *263*, 285–293.
10. Tateno, M., Brabham, C., and DeBolt, S. (2015). Cellulose biosynthesis inhibitors - a multifunctional toolbox. J. Exp. Bot. *67*, 533–542.
11. Scheible, W.R., Eshed, R., Richmond, T., Delmer, D., and Somerville, C. (2001). Modifications of cellulose synthase confer resistance to isoxaben and thiazolidinone herbicides in Arabidopsis Ixr1 mutants. Proc Natl Acad Sci U S A *98*, 10079–10084.
12. Schwessinger, B., Roux, M., Kadota, Y., Ntoukakis, V., Sklenar, J., Jones, A., and

Zipfel, C. (2011). Phosphorylation-dependent differential regulation of plant growth, cell death, and innate immunity by the regulatory receptor-like kinase BAK1. PLoS Genet. *7*, e1002046.

13. Braam, J., Sistrunk, M.L., Polisensky, D.H., Xu, W., Purugganan, M.M., Antosiewicz, D.M., Campbell, P., and Johnson, K.A. (1996). Life in a changing world: TCH gene regulation of expression and responses to environmental signals. Physiol Plant *98*, 909–916.
14. Huffaker, A., Pearce, G., and Ryan, C.A. (2006). An endogenous peptide signal in Arabidopsis activates components of the innate immune response. Proc. Natl. Acad. Sci. U. S. A. *103*, 10098–10103.
15. Yuan, F., Yang, H., Xue, Y., Kong, D., Ye, R., Li, C., Zhang, J., Theprungsirikul, L., Shrift, T., Krichilsky, B., *et al.* (2014). OSCA1 mediates osmotic-stress-evoked Ca2+ increases vital for osmosensing in Arabidopsis. Nature.
16. Haswell, E.S., and Verslues, P.E. (2015). Perspectives on: The response to osmotic challenges: The ongoing search for the molecular basis of plant osmosensing. J. Gen. Physiol. *145*, 389–394.
17. Mousavi, S.A.R., Chauvin, A., Pascaud, F., Kellenberger, S., and Farmer, E.E. (2013). GLUTAMATE RECEPTOR-LIKE genes mediate leaf-to-leaf wound signalling. Nature *500*, 422–6.
18. Nissen, K.S., Willats, W.G.T., and Malinovsky, F.G. (2016). Understanding CrRLK1L Function: Cell Walls and Growth Control. Trends Plant Sci. *xx*, 1–12.
19. Lockhart, J.A. (1965). An analysis of irreversible plant cell elongation. J. Theor. Biol. *8*, 264–275.
20. Levin, D.E. (2011). Regulation of cell wall biogenesis in Saccharomyces cerevisiae: the cell wall integrity signaling pathway. Genetics *189*, 1145–75.
21. Engelsdorf, T., and Hamann, T. (2014). An update on receptor-like kinase involvement in the maintenance of plant cell wall integrity. Ann. Bot. *114*, 1339–47.
22. Stegmann, M., Monaghan, J., Smakowska-Luzan, E., Rovenich, H., Lehner, A., Holton, N., Belkhadir, Y., and Zipfel, C. (2017). The receptor kinase FER is a RALF-regulated scaffold controlling plant immune signaling. *4*, 287–289.
23. Bartels, S., and Boller, T. (2015). Quo vadis, Pep? Plant elicitor peptides at the crossroads of immunity, stress, and development. J. Exp. Bot. *66*, 5183–5193.
24. Huffaker, A., Pearce, G., Veyrat, N., Erb, M., Turlings, T.C.J., Sartor, R., Shen, Z., Briggs, S.P., Vaughan, M.M., Alborn, H.T., *et al.* (2013). Plant elicitor peptides are conserved signals regulating direct and indirect antiherbivore defense. Proc. Natl. Acad. Sci. U. S. A. *110*, 5707–12.
25. Kohorn, B.D., Kobayashi, M., Johansen, S., Riese, J., Huang, L.F., Koch, K., Fu, S., Dotson, A., and Byers, N. (2006). An Arabidopsis cell wall-associated kinase required for invertase activity and cell growth. Plant J *46*, 307–316.
26. Denness, L., McKenna, J.F., Segonzac, C., Wormit, A., Madhou, P., Bennett, M., Mansfield, J., Zipfel, C., and Hamann, T. (2011). Cell wall damage-induced lignin biosynthesis is regulated by a reactive oxygen species- and jasmonic acid-dependent process in Arabidopsis. Plant Physiol. *156*, 1364–74.
27. Hu, K., Cao, J., Zhang, J., Xia, F., Ke, Y., Zhang, H., Xie, W., Liu, H., Cui, Y., Cao, Y., *et al.* (2017). Improvement of multiple agronomic traits by a disease

resistance gene via cell wall reinforcement. Nat. Plants *17009*.

28. de Hoon, M.J.L., Imoto, S., Nolan, J., and Miyano, S. (2004). Open source clustering software. Bioinformatics *20*, 1453–4.
29. Saldanha, A.J. (2004). Java Treeview--extensible visualization of microarray data. Bioinformatics *20*, 3246–8.
30. Law, J.A., and Jacobsen, S.E. Establishing, maintaining and modifying DNA methylation patterns in plants and animals. Nat Rev Genet *11*, 204–220.
31. Robinson, M., and Oshlack, A. (2010). A scaling normalization method for differential expression analysis of RNA-seq data. Genome Biol. *11*, R25.

Fig. 1. Different types of cell wall damage induce similar osmo-sensitive responses. (**A**) Jasmonic acid (JA) and (**B**) Salicylic acid (SA) contents were quantified in 6 d-old Col-0, *bak1-5* and *ixr1-1* seedlings 7 h after treatment with DMSO, Sorbitol (S), Isoxaben (ISX), Driselase (Dri), boiled Dri (bDri) or combinations thereof. Values are means (n = 4) and error bars represent SD. (**C**) Callose depositions in cotyledons have been quantified 24 h after treatment. Values are means (n = 15-20) ± SEM. (**D**) Phloroglucinol-stained lignin in cotyledons 24 h after treatment. Scale bar represents 1 mm. (**E**) Relative *TCH4* expression level in Col-0 seedlings 7 h after treatment. Values are means (n = 3) ± SD. (**F**) Relative *PDF1.2* expression level in Col-0 and *bak1-5* seedlings 7 h after treatment with bDri or Dri compared to non-treated (NT) seedlings. Values are means (n = 3) ± SD. Different letters between treatments of each genotype in (A-E) indicate statistically significant differences according to one-way ANOVA and Tukey's HSD test (α = 0.05). Asterisks in (C) and (F) indicate statistically significant differences between treatments (Student's t-test; * $P < 0.05$; ** $P < 0.01$; *** $P < 0.001$; ns, not significant).

Fig. 2. Phenotypic clustering identifies groups of genes involved in cell wall damage responses. (**A**) Jasmonic acid (JA), (**B**) Salicylic acid (SA) and (**C**) root tip lignification were quantified in 6 d-old mutant seedlings after 7 h (A-B; n = 4, means ± SD) or 12 h (C; $n \geq 10$, means ± SD) of ISX treatment. Values are relative to a wild type control from a representative experiment selected from at least 3 independent experimental repeats. Asterisks indicate statistically significant differences to the wild type (Student's t-test, * $P < 0.05$). Mutant lines are organized in functional groups (RLKs, Receptor-like kinases; *Cr*RLK1Ls, *Catharanthus roseus* RLK1-like kinases; AHKs, Arabidopsis histidine kinases; Ion channels) and individual genotypes described in detail in the Key Resources Table. (**D**) Hierarchical clustering of mutant phenotypes assigns functions in CWI maintenance to candidate genes based on their responses to standardized cell wall damage. Mutant phenotype data from (A-C) and Supplemental Figure S6 (RGI, root growth inhibition) have been normalized to wild type controls and $\log_2$ transformed prior to average linkage clustering. Blue color indicates reduced ISX responses while red color is indicative of increased ISX responses compared to wild type.

Fig. 3. Genetic analysis of *THE1*-dependent cell wall integrity signaling and cross-regulation with *At*Pep1. (**A-C**) Col-0, *mca1, fei2, mca1 fei2, the1-1, the1-1 mca1, the1-1 fei2* and (**D-F**) *the1-4, the1-4 mca1, the1-4 fei2* seedlings were grown for 6 d before treatment with ISX. (A, D) Jasmonic acid (JA), (B, E) Salicylic acid (SA) and (C, F) root tip lignification were quantified after 7 h (JA, SA; n = 4, means ± SD) or 12 h (lignin; $n \geq 17$, means ± SD). (**G**) Relative expression levels of *PROPEP1, 2, 3* and *4* were determined by qRT-PCR after 1 h of treatment with DMSO or ISX in Col-0 seedlings. *PROPEP1* and *3* expression levels were further examined (**H**) after 1 h of treatment with DMSO or ISX in Col-0 and *the1-1* seedlings and (**I**) after 0, 3, 6 and 9 h of treatment in Col-0 seedlings. Values are means (n = 3) ± SD. (**J**) JA and (**K**) SA were quantified in Col-0 seedlings after 7 h of co-treatment with DMSO or ISX and 0, 1, 10 or 100 nM *At*Pep1 (n = 4, means ± SD). (**L**) Root tip lignification in Col-0 after 12 h of co-treatment with DMSO or ISX and *At*Pep1 (0, 1, 10 nM) was visualized by Phloroglucinol staining.

Scale bar represents 200 µm. (**M**) JA and (**N**) SA quantification in Col-0, *pepr1*, *pepr2* and *pepr1 pepr2* after 7 h of co-treatment with DMSO or ISX and 10 nM *At*Pep1 (n = 4, means ± SD). Different letters between genotypes in (A-F) and between treatments of each genotype in (J-N) indicate statistically significant differences according to one-way ANOVA and Tukey's HSD test (α = 0.05). Asterisks in (G-I) indicate statistically significant differences to DMSO-treated controls (Student's *t*-test; * $P < 0.05$).

Fig. 4. Model of the regulatory interactions between the plant CWI maintenance mechanism and pattern triggered immunity. Responses to CWD in Arabidopsis depend on the receptor-like kinases THE1, FEI2, WAK2, MIK2 and ERU and the ion channels MCA1 and MSL2/3 (blue font). THE1, FEI2, WAK2 and MIK2 are localized to the plasma membrane (orange), ERU to the tonoplast (yellow) and MSL2/3 to plastids (green). Signaling downstream of RLKs and ion channels involves signaling molecules Ca^{2+}, reactive oxygen species (ROS), jasmonic acid (JA) and salicylic acid (SA) (all grey spheres). CWD also induces expression of PROPEPs, precursors of elicitor peptides (like *At*Pep1), independent from THE1-dependent CWD-signaling. RLKs required for pattern-triggered immunity such as the *At*Pep receptors PEPR1 / 2 and the co-receptor BAK1 repress CWD-induced phytohormone accumulation (all in red). Interactions between the two signaling cascades regulate downstream responses (including lignin/callose production).

Fig. S1. Analysis of CWD-induced lignification, response to incubation with supernatants from CWD-treatments and CWD-induced root cell bulging. (**A**) CWD-induced lignification was analyzed in cotyledons of 6 d-old *bak1-5* and *ixr1-1* seedlings. Seedlings were treated with DMSO, Sorbitol (S), Isoxaben (ISX), Driselase (Dri), boiled Dri (bDri) or combinations thereof. Cotyledons were stained with Phloroglucinol to visualize lignin deposition 24 h after treatment. Scale bar represents 1 mm. (**B, C**) Extended treatment with ISX or heat-inactivated Driselase generates medium-soluble compounds slightly eliciting hormone accumulation. Col-0 seedlings have been treated with DMSO, Sorbitol (S), Isoxaben (ISX), Driselase (Dri), boiled Dri (bDri) or combinations thereof for 12 or 24 h. Supernatants from DMSO, ISX and ISX/S treatments have been transferred on 6 d-old *ixr1-1* seedlings. Supernatants from DMSO/S, bDri, bDri/S, Dri and Dri/S have been boiled for 10 min and transferred on 6 d-old Col-0 seedlings. (A) Jasmonic acid (JA) and (B) Salicylic acid (SA) were quantified 7 h after start of incubation. Values are means (n = 4) and error bars represent SD. Different letters between treatments of each genotype and time point indicate statistically significant differences according to one-way ANOVA and Tukey's HSD test (α = 0.05). (**D**) Sorbitol co-treatment reduces ISX-induced root cell bulging. 6 d-old WAVE-131YFP seedlings have been treated with DMSO, Sorbitol (S), Isoxaben (ISX) or combinations thereof. After 7 h of treatment images were taken using HC PL APO 10x/0.40 DRY on a Leica SP8. Propidium iodide (PI) staining (1 min, 10 µg/ml) was used to stain the cell walls. The fluorescence related to WAVE-131YFP (green) and PI (red) were used to identify the cell structure. PI and WAVE-131YFP signals largely co-

localize in the epidermis and in root hairs (merge). Arrowheads point to areas with pronounced cell bulging that are magnified in insets. Scale bar represents 250 µm.

Fig. S2. ISX responses in candidate Arabidopsis osmo- and mechano-sensor mutant lines are osmo-sensitive. (**A**) Jasmonic acid (JA) was quantified in 6 d-old *mca1*, *msl2/3*, *msl4/5/6/9/10*, *ahk1*, *ahk2/3, ahk4, glr2.5,* and *the1-4* seedlings after 7 h of treatment with DMSO, Sorbitol (S), Isoxaben (ISX) or combinations thereof. Values are relative to an ISX-treated wild type control (*n* = 3-4, means ± SD). Asterisks indicate statistically significant differences to the wild type (white asterisks) or between treatments (black asterisks; Student's *t*-test, * $P < 0.05$, ** $P < 0.01$). (**B**) Col-0, *mca1*, *ahk2/3*, *msl4/5/6/9/10*, *glr2.5*, Ws-2, *ahk1*, *ahk4, msl2/3* and *the1-4* seedlings were stained with Phloroglucinol 12 h after treatment to visualize root tip lignification. Scale bars represent 200 µm.

Fig. S3. Analysis of hormone accumulation upon mock-treatment, root length and ISX-resistance in Arabidopsis mutant seedlings. (**A**) Jasmonic acid (JA) and (**B**) Salicylic acid (SA) were quantified in 6 d-old mutant seedlings after 7 h mock-treatment (DMSO). Columns represent the average of mean values from 3-4 independent experiments, relative to the respective wild type controls (± SD). Mutant lines are organized in functional groups (RLKs, Receptor-like kinases; *Cr*RLK1Ls, *Catharanthus roseus* RLK1-like kinases; AHKs, Arabidopsis histidine kinases; Ion channels; cf. Fig.2) and individual genotypes described in detail in the Key Resources Table. Absolute amounts of (**C**) JA and (**D**) SA in Col-0 and *fer-5* seedlings treated with DMSO or ISX for 7 h illustrate increased basal hormone levels in *fer-5*. (**E**) Root length and (**F**) ISX-resistance (root growth inhibition, RGI) assays show growth defects and no resistance to ISX-treatment in different mutant seedlings. To assess growth phenotypes, root lengths of 6 day-old wild type and mutant seedlings were measured prior to treatment. Resistance to ISX was determined 24 h after treatment. 100% indicates full sensitivity to ISX-treatment, while 0% indicates complete resistance. Columns represent the average of mean values from 3-8 independent experiments ± SD. Different letters between genotypes in (A, B, E, F) indicate statistically significant differences according to one-way ANOVA and Tukey's HSD test (α = 0.05). Asterisks in (C-D) indicate statistically significant differences to the wild type (Student's *t*-test, * $P < 0.05$).

Fig. S4. Changes in *PROPEP* gene expression after ISX-treatment and root tip lignification upon *At*Pep1 co-treatment. (**A**) 6 d-old Col-0 seedlings were treated with DMSO or ISX. Changes in gene expression were analyzed after 1 h using RNA-Seq (see Supplemental File S1). ISX-induced changes in gene expression of *PROPEP1, 2, 3, 4, 5, 6* and *7* are plotted on a $\log_2$ scale and *P*-values are given next to the individual bars (*n* = 3). (**B**) Root tip lignification in Col-0, *pepr1*, *pepr2* and *pepr1 pepr2* seedlings after 12 h of co-treatment with DMSO or ISX and 10 nM *At*Pep1 was visualized by Phloroglucinol staining. Scale bar represents 200 µm.

Table S1. Gene Ontology (GO) enrichment analysis of genes with ISX-dependent expression changes. Genes with significantly altered expression after 1 h of ISX-treatment (Supplemental File S1) have been analyzed for GO enrichment using the

PANTHER Overrepresentation Test (release 20160715) and the GO Ontology database (Released 2017-02-28) on http://geneontology.org/. Results are filtered by $P < 0.05$ after Bonferroni correction for multiple testing.

Table S2. Primers used in this study.

File S1. RNA-Seq analysis of gene expression changes upon 1 h of ISX-treatment. 6-day old Col-0 and *ixr1-1* seedlings were treated with DMSO or ISX and analyzed by RNA-Seq 1 h after treatment. Raw data from 3 independent biological replicates are shown in the "raw data" tab. 109 transcripts found differentially regulated after ISX- compared to DMSO-treatment ($p < 0.01$) are shown in the tab "Col ISX vs DMSO". Up- or down-regulated transcripts compared to DMSO controls are color-coded orange (up) or blue (down). Fold changes of *PROPEP1, 2, 3, 4, 5, 6* and *7* transcripts are calculated in tab "PROPEP ISX vs. DMSO" and plotted in Supplemental Fig. S4.

CONTACT FOR REAGENT AND RESOURCE SHARING

Further information and requests for resources and reagents should be directed to and will be fulfilled by the Lead Contact, Thorsten Hamann (thorsten.hamann@ntnu.no).

EXPERIMENTAL MODEL AND SUBJECT DETAILS

Arabidopsis thaliana

Arabidopsis thaliana genotypes used in this study were obtained from the labs previously publishing them, or ordered from the Nottingham Arabidopsis Stock Centre (http://arabidopsis.info/). Detailed information is listed in the Key Resources Table. Seedlings were grown in liquid culture as described by [26] with minor modifications. 30 mg of seeds were sterilized by sequential incubation with 70 % ethanol and 50 % bleach on a rotating mixer for 10 min each and washed 3 times with sterile water. Seeds were than transferred into 250 ml erlenmayer flasks containing 125 ml half-strength Murashige and Skoog growth medium (2.1 g/L Murashige and Skoog Basal Medium, 0.5 g/L MES salt and 1 % sucrose at pH 5.7). Seedlings were grown in long-day conditions (16 h light, 22°C / 8 h dark, 18°C) at 150 µmol m^{-2} s^{-1} photon flux density on a IKA KS501 flask shaker at a constant speed of 130 rotations per minute.
Seedlings were treated after 6 days with 600 nM isoxaben (ISX; in DMSO), 0.03% (w/v) Driselase (Dri), 0.03% Dri boiled for 10 min, 300 mM sorbitol (S) and combinations thereof in fresh growth medium. Supernatants from treated Col-0 cultures were incubated with *ixr1-1* seedlings (DMSO, ISX, ISX/S) or boiled for 10 min and incubated with Col-0 seedlings (DMSO/S, bDri, bDri/S, Dri, Dri/S). *At*Pep1 peptide (ATKVKAKQRGKEKVSSGRPGQHN) was obtained from Peptron (Daejeon, South Korea) and dissolved in sterile water.

METHOD DETAILS

Phytohormone Analysis

Jasmonic acid (JA) and salicylic acid (SA) were analyzed as described by (Forcat et al. 2008) with minor modifications. Seedlings were flash-frozen in liquid nitrogen and freeze-dried for 24 h. 6-7 mg aliquots of freeze-dried seedlings were ground with 5 mm stainless steal beads in a Qiagen Tissue Lyser II for 2 min at 25 Hz. Shaking was repeated after addition of 400 µl extraction buffer (10 % methanol, 1 % acetic acid) with internal standards (10 ng Jasmonic-d_5 Acid, 28 ng Salicylic-d_4 Acid; CDN Isotopes, Pointe-Claire, Canada) before samples were incubated on ice for 30 min and centrifuged for 10 min at 16,000 g and 4°C. Supernatants were transferred into fresh tubes and pellets re-extracted with 400 µl extraction buffer without internal standards. Supernatants were combined and centrifuged 3 times to remove all debris prior to LC-MS/MS analysis. An extraction control not containing plant material was treated equally to the plant samples.
Chromatographic separation was carried out on a Shimadzu UFLC XR, equipped with a Waters Cortecs C18 column (2.7 µm, 2.1 x 100 mm). The solvent gradient (acetonitrile (ACN) / water with 0.1 % formic acid each) was adapted to a total run time of 7 min: 0-4 min 20 % to 95 % ACN, 4-5 min 95 % ACN, 5-7 min 95 % to 20 % ACN; flow rate 0.4 ml / min. For hormone identification and quantification an AB SCIEX Triple Quad 5500 system was used. Mass transitions were: JA 209 > 59, D_5-JA 214 > 62, SA 137 > 93, D_4-SA 141 > 97.

Callose Analysis

Seedlings were sampled 24 h after treatment and placed in 70 % (v/v) ethanol. For callose staining, samples were incubated in 0.07 M sodium phosphate buffer pH 9 for 30 min and in 0.005 % (w/v) aniline blue (in 0.07 M sodium phosphate buffer pH 9) for 60 min. Samples were washed with water, mounted in 50 % (v/v) glycerol and analyzed under a Nikon Eclipse E800 microscope using a UV-2A filter (EX 330-380 nm, DM 400 nm, BA 420 nm). Images were taken at 10x magnification and callose depositions quantified using ImageJ software.

Lignin Analysis

Lignification was investigated 12 h (root tips) and 24 h (cotyledons) after start of treatments. Lignin was detected with phloroglucinol-HCL as described [26]. Seedlings were photographed using a Zeiss Axio Zoom.V16 stereomicroscope. To assess the extent of lignin production in root tips, phloroglucinol-stained areas and the total root area imaged were quantified using ImageJ (the same root length was maintained in all images taken). The relative lignified area was plotted as fold change compared to wild type root tips.

Root Measurements

Absolute root lengths were measured immediately prior to ISX treatment (0 h) to examine root growth phenotypes and 24 h after start of treatment to determine ISX-dependent root growth inhibition (RGI). For calculation of %RGI the following formula was applied: [1 - (ISX 24h - ISX 0h) / (mock 24h - mock 0h)]*100.

Hierarchical Cluster Analysis

Hierarchical Clustering of ISX-dependent phenotypes was performed with Cluster 3.0

using the C Clustering Library v1.52 [28]. All data of mutant seedlings was normalized to their corresponding wild type control. Log_2 transformed data was then used for average linkage clustering with an uncentered correlation similarity metric. Results were depicted using Java TreeView v1.1.6r4 [29] and color-coded blue (less than in wild type) or red (more than in wild type).

Semi-quantitative RT-PCR

Total RNA was isolated using a Qiagen RNeasy Mini Kit in combination with DNaseI treatment according to manufacturer instructions (www.quiagen.com). For reverse transcription the Qiagen Omniscript Kit and oligo(dT) primers were used according to the manufacturers´ instructions. Sequences of primers used for amplification (*ACT1, GLR2.5*) are listed in Supplemental Table S2.

qRT-PCR

Total RNA was isolated using a Spectrum Plant Total RNA Kit (Sigma-Aldrich). 2 µg of total RNA were treated with RQ1 RNase-Free DNase (Promega) and processed with the ImProm-II Reverse Transcription System (Promega) for cDNA synthesis. qRT-PCR was performed using a LightCycler 480 SYBR Green I Master (Roche) and primers (Supplemental Table S2) diluted according to manufacturer specifications. Four different reference genes (*PP2A, ACT2, UBA1, GRF2*) were examined to identify one exhibiting stable expression during ISX-treatment. *ACT2* was the most stable one and used in all experiments as reference.

RNA-Seq

Total RNA was extracted using a Spectrum Plant Total RNA Kit (Sigma-Aldrich). RNA concentration was measured using a Qubit RNA HS Assay Kit (Thermo Fisher Scientific) and integrity assessed using a Agilent RNA 6000 Pico Kit. RNA Seq libraries were prepared using a TruSeq Stranded mRNA Kit (Illumina) according to the manufacturer's instructions. 500 ng total RNA was used as starting material.
First, index barcodes were ligated for identification of individual samples. mRNA purification, fragmentation and cDNA synthesis has been performed as described in (Ren et al. 2015). Exonuclease / polymerase was used to produce blunted overhangs. Illumina SR adapter oligonucleotides were ligated to the cDNA after 3' end adenylation. DNA fragments were enriched by 15 cycles of PCR reaction. The libraries were purified using the AMPure XP (Beckman Coulter), quantitated by qPCR using a KAPA Library Quantification Kit (Kapa Biosystems) and validated using a Agilent High Sensitivity DNA Kit on a Bioanalyzer. The size range of the DNA fragments were measured to be in the range of 200-700 bp and peaked around 296 bp. Libraries were normalized and pooled to 2.2 pM and subjected to clustering on NextSeq 500 high output flowcells. Finally single read sequencing was performed for 75 cycles on a NextSeq 500 instrument (Illumina) according to the manufacturer instructions. Base-calling has been performed on the NS500 instrument by Illumina RTA v2.4.6. FASTQ files were generated using bcl2fastq2 Conversion Software v1.8.4. Each FASTQ file was subjected to quality control trough fastQC v11.1 before technical replicates were combined and an average of 13.1 million reads was produced for each library. The reads were then aligned to the *A. thaliana* genome (Ensembl v82) with STAR v2.4.1 in two-pass mode. On average,

96.2% of the reads aligned to the genome. The reads that aligned uniquely to the genome were aggregated into gene counts with FeatureCounts v1.4.6 using the genome annotations defined in Ensembl v82. Of the 32000 genes defined in the gene model, a total of 20750 genes were left for analysis after filtering out genes with a CPM (counts-per-million) value less than one in two or more samples.
The filtered gene count table was used as input to the Voom method [30] of the Limma R package v3.26.9 for differential expression. The samples were normalized using the TMM [31] method before a linear model was defined. Differential expression between groups were tested by empirical Bayesian moderated *t*-tests and *P*-values were corrected for multiple testing by the Benjamini-Hochberg false discovery rate adjustment. Statistical significance of pairwise comparisons was determined using a Student's *t*-test.

QUANTIFICATION AND STATISTICAL ANALYSIS

Statistical significance was assed using either Student's *t*-test or one-way ANOVA followed by post-hoc analysis with Tukey's HSD test. Statistical details of experiments are specified in the figure legends. Statistically significant differences are indicated by * $P < 0.05$, ** $P < 0.01$, *** $P < 0.001$ for Student's *t*-test and different letters for one-way ANOVA / Tukey's HSD test at $\alpha = 0.05$. All statistical analyses were performed in IBM SPSS Statistics v24.

DATA AND SOFTWARE AVAILABILITY

Data Resource
Raw data from RNA-Seq analysis are listed in Supplemental File S1 and will be deposited at the Bio-analytic Resource for Plant Biology.

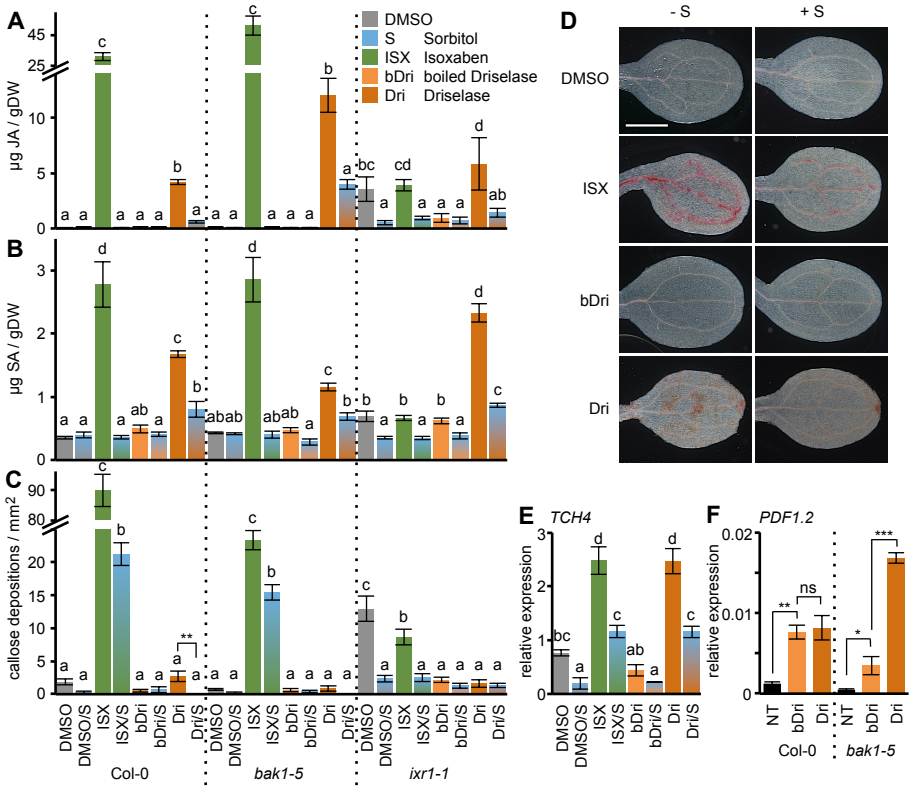
A
B
C
D
E
F
DMSO
S Sorbitol
ISX Isoxaben
bDri boiled Driselase
Dri Driselase
µg JA / gDW
µg SA / gDW
callose depositions / mm2
- S
+ S
DMSO
ISX
bDri
Dri
TCH4
PDF1.2
relative expression
NT
bDri
Dri
ns
Col-0
bak1-5
ixr1-1

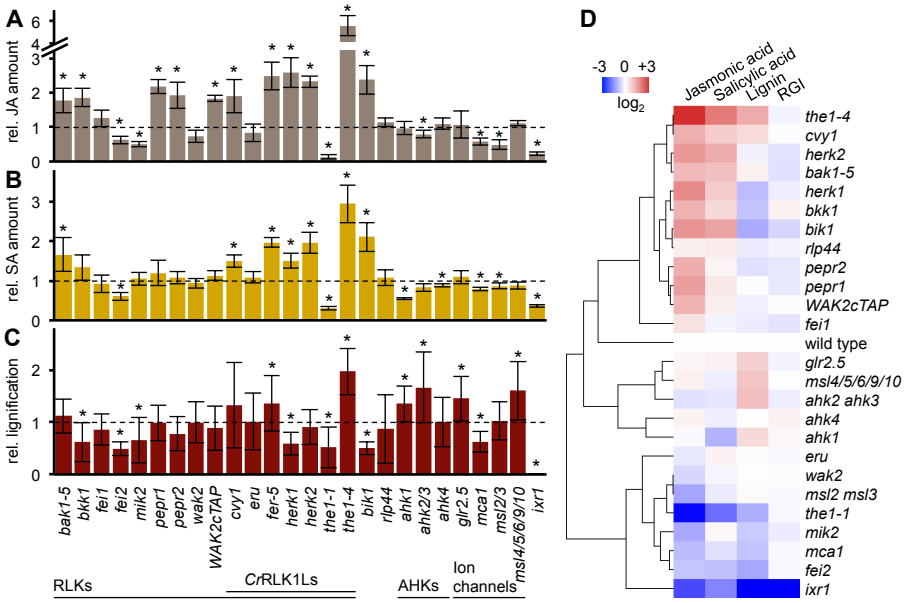
A
rel. JA amount
B
rel. SA amount
C
rel. lignification
bak1-5
bkk1
fei1
fei2
mik2
pepr1
pepr2
wak2
WAK2cTAP
cvy1
eru
fer-5
herk1
herk2
the1-1
the1-4
bik1
rlp44
ahk1
ahk2/3
ahk4
glr2.5
mca1
msl2/3
msl4/5/6/9/10
ixr1
RLKs
CrRLK1Ls
AHKs
Ion channels
D
-3 0 +3
log2
Jasmonic acid
Salicylic acid
Lignin
RGI
the1-4
cvy1
herk2
bak1-5
herk1
bkk1
bik1
rlp44
pepr2
pepr1
WAK2cTAP
fei1
wild type
glr2.5
msl4/5/6/9/10
ahk2 ahk3
ahk4
ahk1
eru
wak2
msl2 msl3
the1-1
mik2
mca1
fei2
ixr1

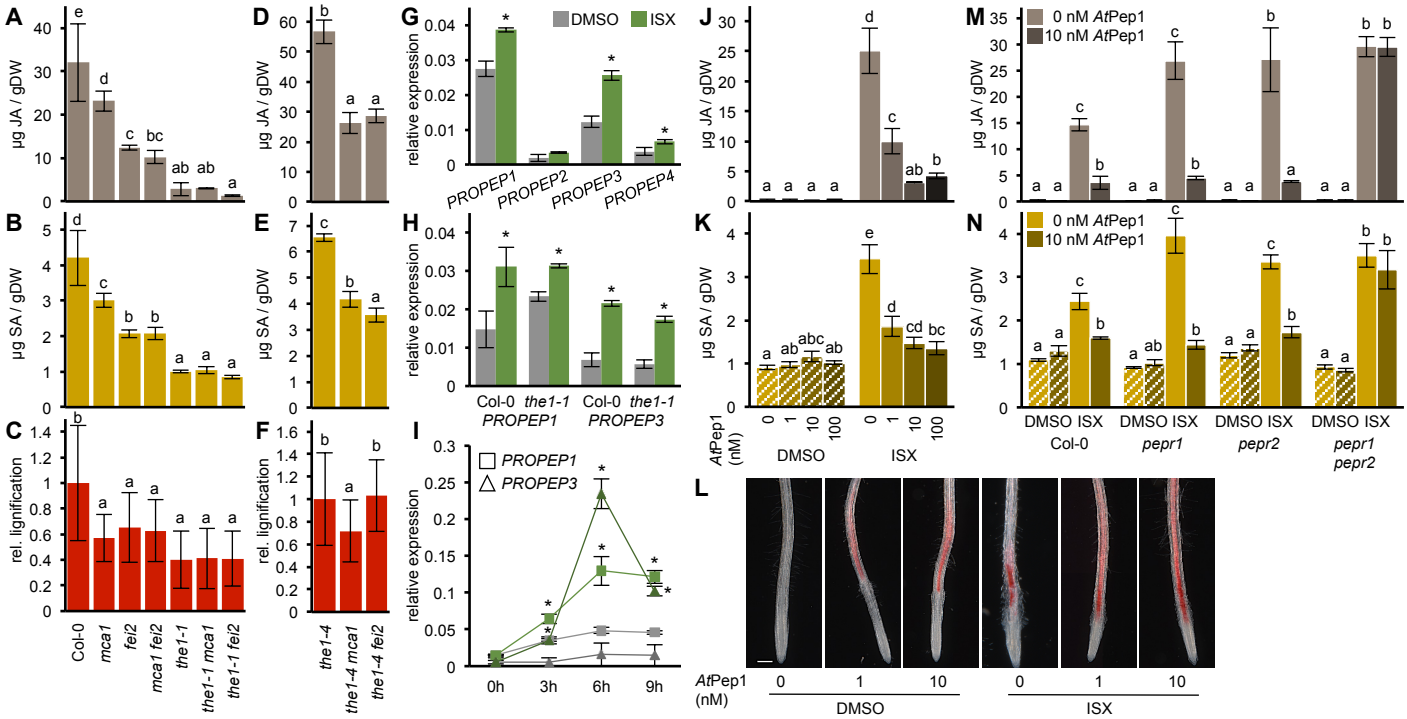
A
µg JA / gDW
B
µg SA / gDW
C
rel. lignification
Col-0
mca1
fei2
mca1 fei2
the1-1
the1-1 mca1
the1-1 fei2
D
E
F
the1-4
the1-4 mca1
the1-4 fei2
G
DMSO
ISX
relative expression
PROPEP1
PROPEP2
PROPEP3
PROPEP4
H
Col-0 the1-1
PROPEP1
Col-0 the1-1
PROPEP3
I
PROPEP1
PROPEP3
0h
3h
6h
9h
J
K
AtPep1 (nM)
DMSO
ISX
L
M
0 nM AtPep1
10 nM AtPep1
N
DMSO ISX
Col-0
pepr1
pepr2
pepr1 pepr2

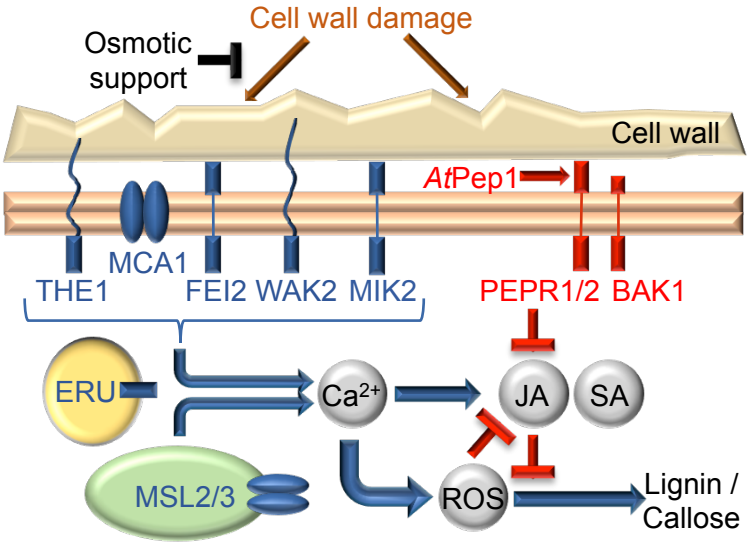
Osmotic support
Cell wall damage
Cell wall
AtPep1
MCA1
THE1
FEI2
WAK2
MIK2
PEPR1/2
BAK1
ERU
Ca2+
JA
SA
MSL2/3
ROS
Lignin / Callose